Inorganic Chemistry

Communication

Binding of a Fatty Acid-Functionalized Anderson-Type Polyoxometalate to Human Serum Albumin

Aleksandar Bijelic, Anatolie Dobrov, Alexander Roller, and Annette Rompel*

Cite This: *Inorg. Chem.* 2020, 59, 5243−5246

Read Online

ACCESS | Metrics & More | Article Recommendations | Supporting Information

ABSTRACT: The Anderson-type hexamolybdoaluminate functionalized with lauric acid (LA), $(TBA)_3[Al(OH)_3Mo_6O_{18}\{(OCH_2)_3CNHCOC_{11}H_{23}\}] \cdot 9H_2O$ (TBA-AlMo$_6$-LA, where TBA = tetrabutylammonium), was prepared via two synthetic routes and characterized by thermogravimetric and elemental analyses, mass spectrometry, IR and ^1H NMR spectroscopy, and powder and single-crystal X-ray diffraction. The interaction of TBA-AlMo$_6$-LA with human serum albumin (HSA) was investigated via fluorescence and circular dichroism spectroscopy. The results revealed that TBA-AlMo$_6$-LA binds strongly to HSA (63% quenching at an HSA/TBA-AlMo$_6$-LA ratio of 1:1), exhibiting static quenching. In contrast to TBA-AlMo$_6$-LA, the nonfunctionalized polyoxometalate, $Na_3(H_2O)_6[Al(OH)_6Mo_6O_{18}] \cdot 2H_2O$ (AlMo$_6$), showed weak binding toward HSA (22% quenching at a HSA/AlMo$_6$ ratio of 1:25). HSA binding was confirmed by X-ray structure analysis of the HSA-Myr-AlMo$_6$-LA complex (Myr = myristate). These results provide a promising lead for the design of novel polyoxometalate-based hybrids that are able to exploit HSA as a delivery vehicle to improve their pharmacokinetics and bioactivity.

Polyoxometalates (POMs) are defined as polynuclear metal oxide clusters that exhibit versatile structures and properties. They have gained attention because of their potential applications in the fields of catalysis,[1] materials science,[2] medicine,[3−5] and macromolecular crystallography.[6] Particularly in the medical sector, POMs have made remarkable progress because a series of compounds, including purely inorganic and organically modified POMs, show promising antitumor, antiviral, and antibacterial effects.[4,5] However, the mechanisms of action and selectivity remain elusive.[7,8] Thus, it is of utmost importance to study the interactions of POMs with biomacromolecules to gain a deeper understanding of their biological activity. Human serum albumin (HSA) is the most abundant protein in human blood plasma and responsible for maintenance of the oncotic pressure and the transport of endogenous and exogenous ligands, such as fatty acids (FAs), metal ions, and a plethora of pharmaceutical compounds.[9] Therefore, HSA might play an important role in the fate of biologically active POMs when injected into blood. Because HSA possesses up to seven binding sites for FAs, functionalization of a given POM with a FA should enhance its binding affinity toward the transport protein and thus modulate its pharmacokinetic behavior.[10] The literature on FA-functionalized (or long-alkyl-chain-containing) POMs is scarce and limited to structures that self-assemble into POM-based vesicles (Table S1). Herein we describe the synthesis, characterization, and crystal structure of $(TBA)_3[Al(OH)_3Mo_6O_{18}\{(OCH_2)_3CNHCOC_{11}H_{23}\}] \cdot 9H_2O$ (TBA-AlMo$_6$-LA, where TBA = tetrabutylammonium), an Anderson-type hexamolybdoaluminate functionalized with lauric acid ($C_{12}H_{24}O_2$, LA) over a tris(hydroxymethyl)-aminomethane (Tris) moiety.[11,12] Postmodification of single-side-functionalized Anderson-type POMs represents a smart strategy to synthesize hybrid compounds with attractive functionalities.[13] TBA-AlMo$_6$-LA is, to the best of our knowledge, the first single-sided Anderson-type POM carrying a FA. The interactions of the TBA and sodium salt of AlMo$_6$-LA and the purely inorganic POM, $Na_3(H_2O)_6[Al(OH)_6Mo_6O_{18}] \cdot 2H_2O$ (AlMo$_6$), with HSA were investigated by fluorescence and circular dichroism (CD) spectroscopy, revealing that LA attachment enhances the affinity of the POM toward HSA. HSA binding of TBA-AlMo$_6$-LA was confirmed by determining the crystal structure of the HSA-Myr-AlMo$_6$-LA complex at a moderate resolution of 3.0 Å.

TBA-AlMo$_6$-LA was prepared via two synthetic routes, which are shown in Scheme 1. In route A, tris-(hydroxymethyl)lauroylamidomethane (Tris-lauroyl) is synthesized first and then attached to the unmodified AlMo$_6$ via a condensation reaction. To avoid the double-sided product (i.e., functionalization from both sides of the POM), the latter reaction had to take place in an aqueous solution, which in this case did also contain dimethyl sulfoxide (DMSO).[13b,14] Route B starts from the Tris-modified Anderson-type polyoxomolybdate $(TBA)_3[Al(OH)_3Mo_6O_{18}\{(OCH_2)_3CNH_2\}] \cdot 7H_2O$, which is linked to LA by an amidation reaction between the acyl chloride group of lauroyl chloride and the amine group of Tris (see the Supporting Information). Route 2 was more straightforward and achieved higher yields than route 1 (77% vs 49%).

Scheme 1. Synthetic Routes To Prepare AlMo$_6$-LA[a]
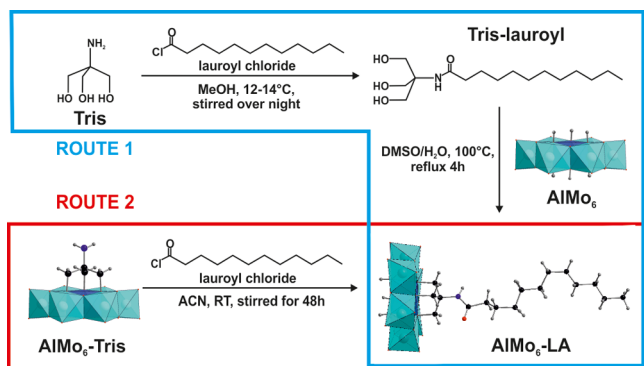
[a]MeOH = methanol, DMSO = dimethyl sulfoxide, ACN = acetonitrile, and RT = room temperature.

The crystal structure of TBA-AlMo$_6$-LA was determined by single-crystal X-ray diffraction and contains one molecule of AlMo$_6$-LA, three TBA countercations, and nine water molecules. Experimental details, crystal parameters, and bond lengths are summarized in Tables S2 and S3. The geometry of the inorganic framework is based on the common Anderson structure: one central {AlO$_6$} octahedron is connected to six hexagonally arranged edge-sharing {MoO$_6$} octahedra via six μ_3-O atoms. The Tris-lauroyl group is directly attached to three μ_3-O atoms via its Tris functionality, whereby the alkyl chain adopts a rather stretched conformation. The crystal packing can be described as alternate layers of AlMo$_6$-LA and TBA molecules (Figure 1). The POM layer consists of pairs of
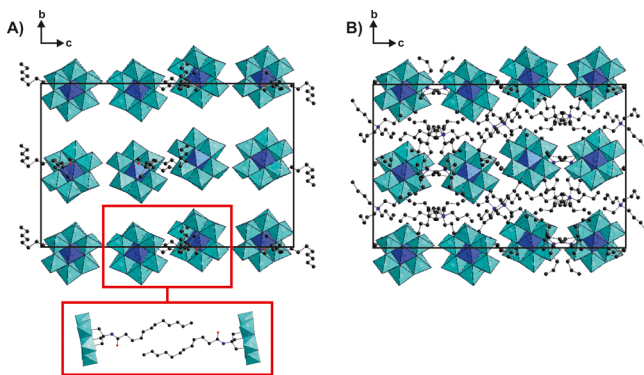

Figure 1. Crystal packing of TBA-AlMo$_6$-LA, viewed along the *a* axis. (A) Crystal packing with omitted TBA countercations. The red inset depicts a pair of AlMo$_6$-LA molecules from another perspective to highlight the hydrophobic interactions between them. (B) Crystal packing with omitted LA chains. A comparison of parts A and B indicates the alternating layers of AlMo$_6$-LA and TBA molecules. Lattice water molecules are omitted for clarity. Color code: cyan octahedra, {MoO$_6$}; blue octahedra, {AlO$_6$}; blue spheres, N; red spheres, O; black spheres, C.

AlMo$_6$-LA molecules whose alkyl chains interact hydrophobically with each other (Figure 1A, inset). In addition, the alkyl chains of the POMs interact hydrophobically with those of the TBA cations, leading to the connection of TBA with the POM layer.

The number of lattice water molecules per unit of TBA-AlMo$_6$-LA (=9 H$_2$O) was determined by thermogravimetric analysis (TGA) and is in accordance with the results of the X-ray experiment (Figure S1). TBA-AlMo$_6$-LA was further

characterized by elemental analysis (see the Supporting Information), powder X-ray diffraction (Figure S2), attenuated-total-reflectance IR (ATR-IR; Figure S3), and ^{1}H NMR spectroscopy (Figure S4). All experimental results confirmed the successful synthesis of TBA-AlMo$_6$-LA.

The interaction of TBA-AlMo$_6$-LA with HSA was analyzed by fluorescence spectroscopy. HSA contains a single tryptophan residue (Trp214) that is responsible for most of the protein's intrinsic fluorescence (tyrosine residues also contribute to the protein's fluorescence). Upon excitation with UV light, HSA fluoresces in the region of 300−400 nm. This fluorescence can be quenched by binding events due to the susceptibility of Trp214 to changes in its microenvironment.[15] The fluorescence spectra of HSA in the presence of increasing concentrations of TBA-AlMo$_6$-LA show that the hybrid POM attenuated the fluorescence efficiently, which indicates that the binding of TBA-AlMo$_6$-LA has affected the microenvironment of Trp214 (Figure 2). In addition, binding of TBA-AlMo$_6$-LA

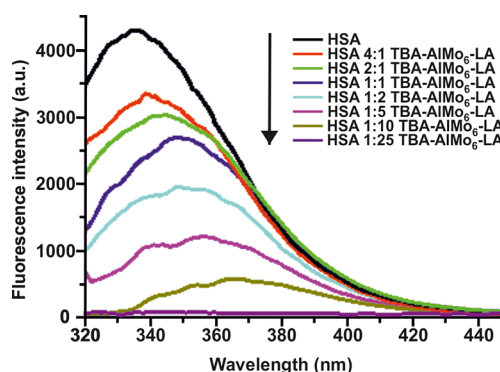**Figure 2.** Fluorescence quenching spectra of HSA at different concentrations of TBA-AlMo$_6$-LA. Spectra were measured at 303 K. The excitation wavelength was 270 nm, and the emission wavelength was in the range of 320−450 nm. c(HSA) = 5 μM, and c(TBA-AlMo$_6$-LA) = 1.25, 2.5, 5, 10, 25, 50, and 125 μM, respectively. All samples were dissolved in 20 mM potassium phosphate (pH 7.4) and 150 mM potassium chloride.

causes a bathochromic shift of the emission maximum, suggesting that the polarity of the microenvironment of Trp214 was increased, most probably because of TBA-AlMo$_6$-LA-induced conformational changes around Trp214 that made the residue more solvent-exposed.

Fluorescence spectra were also recorded for pristine POM (AlMo$_6$), TBA, LA, and the sodium salt of AlMo$_6$-LA (Na-AlMo$_6$-LA) as a control (Figures S5−S7). AlMo$_6$ showed weak quenching because only a 25-fold excess of POM produced a notable reduction in fluorescence (Figure S5). LA exhibited no quenching at all but instead showed a hyperchromic effect (Figure S6A). This effect was most probably caused by LA-mediated conformational changes within HSA.[16] TBA had almost no effect on the protein's fluorescence (Figure S6B), and the quenching effect of Na-AlMo$_6$-LA was very similar to that of the TBA salt reported here (Figure S7), indicating that quenching by the countercations was negligible.

Quenching can occur by different mechanisms (dynamic and/or static quenching), which are characterized by their distinct behavior at increasing temperature. Therefore, fluorescence quenching was evaluated at three different temperatures (303, 308, and 310.5 K; Figure S8). The

quenching mechanism was deduced by the Stern−Volmer equation:[17]

$$F_0/F = 1 + K_{SV}[Q] \qquad (1)$$

where F_0 and F are the fluorescence intensities in the absence and presence of the quencher, respectively, $[Q]$ is the concentration of the quencher, and K_{SV} is the Stern−Volmer constant. The Stern−Volmer plots of the HSA-AlMo$_6$-LA system are linear, and the slopes ($=K_{SV}$) decrease with increasing temperature (Figure S9). This indicates static quenching and thus the formation of a stable HSA-AlMo$_6$-LA complex.

To determine the association constant (K_A) and the number of binding sites (n) for TBA-AlMo$_6$-LA, the double logarithm Stern−Volmer equation was used:[17]

$$\log[(F_0 - F)/F] = \log K_A + n \log [Q] \qquad (2)$$

The results obtained from the modified Stern−Volmer plots at different temperatures (Figure S10) are summarized in Table S4. TBA-AlMo$_6$-LA binded to HSA in a ratio of 1:1 at every tested temperature.

Subsequent CD spectroscopy confirmed the results of the fluorescence quenching experiment (see Figure S11 and Table S5). The secondary structure (i.e., α-helical content) of HSA changed significantly with increasing concentration of TBA-AlMo$_6$-LA. LA also perturbed the protein's secondary structure but to a lesser extent compared to TBA-AlMo$_6$-LA, whereas the unmodified AlMo$_6$ caused observable effects only at high concentrations (25-fold excess).

The soaking of preformed HSA-Myr crystals (Myr = myristate; the FA was required to form HSA crystals) with TBA-AlMo$_6$-LA led to the crystal structure of HSA-Myr-AlMo$_6$-LA with two bound POM molecules (Figure 3; for crystallographic details, see the Supporting Information and Table S6). Despite the moderate resolution of the complex structure (3.0 Å) and the low occupancy of the AlMo$_6$-LA molecules (~0.2−0.3), the inorganic framework of each POM was clearly visible in the electron density map (Figure S12A). However, because of the flexible nature of the alkyl chain, the Tris-lauroyl group of each POM could not be detected unambiguously. Weak and partial electron density (only visible at a contour level of 0.3σ) was found for the Tris-lauroyl group of only one AlMo$_6$-LA molecule, whereas no density was detected for that of the second POM (thus the organic moiety of this POM was not modeled). The former AlMo$_6$-LA molecule is situated within the interdomain cleft of HSA, which is located between domains IB and IIIA (Figures 3A and S12B), whereas the other POM molecule is bound peripherally to HSA within a crystal contact. Owing to its peripheral location, the second AlMo$_6$-LA site represents a crystallographic artifact rather than a relevant POM binding site. Thus, HSA appears to possess only one AlMo$_6$-LA binding site, which is in accordance with the results from the modified Stern−Volmer analysis. The binding site of AlMo$_6$-LA is dominated by hydrophobic and positively charged residues (Figure S12C). The inorganic core of AlMo$_6$-LA is mainly stabilized by arginine 197 (R197) and histidine 146 (H146) via electrostatic interactions and by asparagine 109 (N109) via hydrogen bonding (Figure 3B). However, lysine 190 (K190) and arginine 114 (R114), which are located near the AlMo$_6$ framework, could also contribute to POM binding. Despite both residues being rather distant from the POM, they are highly flexible and could therefore move toward the POM to
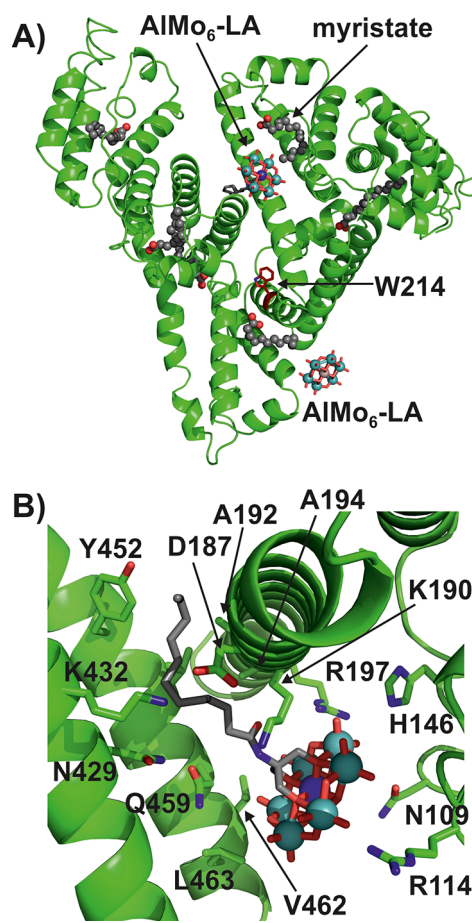

Figure 3. Crystal structure of HSA-Myr-AlMo$_6$-LA. (A) Overall structure of the complex. (B) Binding site of AlMo$_6$-LA. The protein is presented as a green cartoon, with residues that are involved in POM binding being shown as sticks, whereas the POM is illustrated as a ball-and-stick presentation. Color code: green (protein), C; gray (POM), C; blue (stick), N; blue (sphere), Al; cyan, Mo; red, O.

exhibit electrostatic interactions, which we believe would be the case if the occupancy of the POM was higher. The amine center of the Tris-lauroyl group is hydrogen-bonded to glutamine 459 (Q459), whereas the alkyl chain exhibits hydrophobic interactions with alanine 192/194 (A192/A194), valine 462 (V462), the aromatic ring of tyrosine 452 (Y452), and the aliphatic groups of aspartic acid 187 (D187) and lysine 190 and 432 (K190/K432). More details about the data collection, crystal structure elucidation, and POM binding are given in Table S6 and the Supporting Information.

The results presented here clearly demonstrate that the attachment of a FA to the Anderson-type core, which was shown to exhibit anticancer activity,[18] clearly increases the affinity of the POM toward HSA. This improved binding capability of TBA-AlMo$_6$-LA toward HSA protects the POM, inter alia, from premature degradation and excretion, leading to increased bioavailability. Furthermore, the selectivity of the hybrid for cancer cells might be increased due to the enhanced permeability and retention effect, which is responsible for the HSA-mediated transportation and subsequent passive accumulation of a series of drugs within cancer cells.[19]

In conclusion, we have synthesized and characterized a FA-functionalized Anderson-type polyoxomolybdate exhibiting the expected remarkable HSA-binding properties. This work could provide a rational design for bioactive POMs with enhanced

pharmacokinetic properties by exploiting HSA as a delivery vehicle.

ASSOCIATED CONTENT

Supporting Information

The Supporting Information is available free of charge at https://pubs.acs.org/doi/10.1021/acs.inorgchem.9b03407.

Experiments, general characterizations, X-ray diffraction data, TGA, and ^{1}H NMR and ATR-IR spectroscopy (PDF)

Accession Codes

CCDC 1944363 contains the supplementary crystallographic data for this paper. These data can be obtained free of charge via www.ccdc.cam.ac.uk/data_request/cif, or by emailing data_request@ccdc.cam.ac.uk, or by contacting The Cambridge Crystallographic Data Centre, 12 Union Road, Cambridge CB2 1EZ, UK; fax: +44 1223 336033.

AUTHOR INFORMATION

Corresponding Author

Annette Rompel − *Fakultät für Chemie, Institut für Biophysikalische Chemie, Universität Wien, 1090 Wien, Austria;* orcid.org/0000-0002-5919-0553; Email: annette.rompel@univie.ac.at; http://www.bpc.univie.ac.at

Authors

Aleksandar Bijelic − *Fakultät für Chemie, Institut für Biophysikalische Chemie, Universität Wien, 1090 Wien, Austria*
Anatolie Dobrov − *Fakultät für Chemie, Institut für Biophysikalische Chemie, Universität Wien, 1090 Wien, Austria*
Alexander Roller − *Fakultät für Chemie, Zentrum für Röntgenstrukturanalyse, Universität Wien, 1090 Wien, Austria*

Complete contact information is available at:
https://pubs.acs.org/10.1021/acs.inorgchem.9b03407

Author Contributions

The manuscript was written through contributions of all authors.

Notes

The authors declare no competing financial interest.

REFERENCES

(1) Wang, S.-S.; Yang, G.-Y. Recent Advances in Polyoxometalate-Catalyzed Reactions. *Chem. Rev.* **2015**, *115* (11), 4893−4962.

(2) Casañ-Pastor, N.; Gómez-Romero, P. Polyoxometalates: From Inorganic Chemistry to Materials Science. *Front. Biosci., Landmark Ed.* **2004**, *9*, 1759−1770.

(3) Rhule, J. T.; Hill, C. L.; Judd, D. A.; Schinazi, R. F. Polyoxometalates in Medicine. *Chem. Rev.* **1998**, *98* (1), 327−358.

(4) Bijelic, A.; Aureliano, M.; Rompel, A. The Antibacterial Activity of Polyoxometalates: Structures, Antibiotic Effects and Future Perspectives. *Chem. Commun.* **2018**, *54* (10), 1153−1169.

(5) (a) Bijelic, A.; Aureliano, M.; Rompel, A. Polyoxometalates as Potential Next-Generation Metallodrugs in the Combat Against Cancer. *Angew. Chem., Int. Ed.* **2019**, *58* (10), 2980−2999. (b) Bijelic, A.; Aureliano, M.; Rompel, A. Im Kampf gegen Krebs: Polyoxometallate als nächste Generation metallhaltiger Medikamente. *Angew. Chem.* **2019**, *131* (10), 3008−3029.

(6) (a) Bijelic, A.; Rompel, A. The Use of Polyoxometalates in Protein Crystallography - An Attempt to Widen a Well-Known Bottleneck. *Coord. Chem. Rev.* **2015**, *299*, 22−38. (b) Bijelic, A.; Rompel, A. Polyoxometalates - More than a phasing tool in protein crystallography. *ChemTexts* **2018**, *4* (3), 10. (c) Bijelic, A.; Rompel, A. Ten good reasons for the use of the tellurium-centered Anderson-Evans polyoxotungstate in protein crystallography. *Acc. Chem. Res.* **2017**, *50* (6), 1441−1448.

(7) Judd, D. A.; Nettles, J. H.; Nevins, N.; Snyder, J. P.; Liotta, D. C.; Tang, J.; Ermolieff, J.; Schinazi, R. F.; Hill, C. L. Polyoxometalate HIV-1 Protease Inhibitors. A New Mode of Protease Inhibition. *J. Am. Chem. Soc.* **2001**, *123* (5), 886−897.

(8) Hasenknopf, B. Polyoxometalates: Introduction to a Class of Inorganic Compounds and Their Biomedical Applications. *Front. Biosci., Landmark Ed.* **2005**, *10* (1−3), 275.

(9) Carter, D. C.; Ho, J. X. Structure of Serum Albumin. *Adv. Protein Chem.* **1994**, *45*, 153−203.

(10) Simard, J. R.; Zunszain, P. A.; Hamilton, J. A.; Curry, S. Location of High and Low Affinity Fatty Acid Binding Sites on Human Serum Albumin Revealed by NMR Drug-Competition Analysis. *J. Mol. Biol.* **2006**, *361* (2), 336−351.

(11) Blazevic, A.; Rompel, A. The Anderson-Evans Polyoxometalate: From Inorganic Building Blocks via Hybrid Organic-Inorganic Structures to Tomorrows "Bio-POM". *Coord. Chem. Rev.* **2016**, *307*, 42−64.

(12) Gumerova, N. I.; Blazevic, A.; Caldera Fraile, T.; Roller, A.; Giester, G.; Rompel, A. Synthesis and Characterization of Hybrid Anderson Hexamolybdoaluminates(III) Functionalized with Indometacin or Cinnamic Acid. *Acta Crystallogr., Sect. C: Struct. Chem.* **2018**, *74* (11), 1378−1383.

(13) (a) Wu, P.; Yin, P.; Zhang, J.; Hao, J.; Xiao, Z.; Wei, Y. Single-Side Organically Functionalized Anderson-Type Polyoxometalates. *Chem. - Eur. J.* **2011**, *17* (43), 12002−12005. (b) Ai, H.; Wang, Y.; Li, B.; Wu, L. Synthesis and Characterization of Single-Side Organically Grafted Anderson-Type Polyoxometalates. *Eur. J. Inorg. Chem.* **2014**, *2014* (17), 2766−2772. (c) Lin, C.-G.; Chen, W.; Long, D.-L.; Cronin, L.; Song, Y.-F. Step-by-Step Covalent Modification of Cr-Templated Anderson-Type Polyoxometalates. *Dalton Trans.* **2014**, *43* (23), 8587−8590.

(14) Gumerova, N. I.; Roller, A.; Rompel, A. Synthesis and Characterization of the First Nickel(II)-Centered Single-Side Tris-Functionalized Anderson-Type Polyoxomolybdate. *Eur. J. Inorg. Chem.* **2016**, *2016* (36), 5507−5511.

(15) Teresa Montero, M.; Hernández, J.; Estelrich, J. Fluorescence Quenching of Albumin. A Spectrofluorimetric Experiment. *Biochem. Educ.* **1990**, *18* (2), 99−101.

(16) Kragh-Hansen, U.; Hellec, F.; de Foresta, B.; le Maire, M.; Møller, J. V. Detergents as Probes of Hydrophobic Binding Cavities in Serum Albumin and Other Water-Soluble Proteins. *Biophys. J.* **2001**, *80* (6), 2898−2911.

(17) Lakowicz, J. R. *Principles of Fluorescence Spectroscopy*, 3rd ed., corr. 4th print; Springer: New York, 2010.

(18) Liu, Y.; Tian, S.; Liu, S.; Wang, E. In Vitro Inhibitory Effect of Polyoxometalates on Human Tumor Cells. *Transition Met. Chem.* **2005**, *30* (1), 113−117.

(19) Kratz, F. Albumin as a Drug Carrier: Design of Prodrugs, Drug Conjugates and Nanoparticles. *J. Controlled Release* **2008**, *132* (3), 171−183.